NASA Technical Memorandum 85894

USAAVSCOM Technical Report 84-A-3

Navier-Stokes Calculations for the Vortex Wake of a Rotor in Hover

C.H. Liu, J.L. Thomas, and C. Tung

May 1984

National Aeronautics and Space Administration

United States Army Aviation Systems Command

NASA Technical Memorandum 85894

USAAVSCOM Technical Report 84-A-3

Navier-Stokes Calculations for the Vortex Wake of a Rotor in Hover

C. H. Liu
J. L. Thomas, Langley Research Center, Hampton, Virginia
C. Tung, Aeromechanics Laboratory, U. S. Army Research and Technology Laboratories-AVSCOM
Ames Research Center, Moffett Field, California

NASA
National Aeronautics and
Space Administration

Ames Research Center
Moffett Field, California 94035

United States Army
Aviation Systems
Command
St. Louis, Missouri 63120

NAVIER-STOKES CALCULATIONS FOR THE VORTEX WAKE OF A ROTOR IN HOVER

C. H. Liu* and J. L. Thomas*
NASA Langley Research Center
Hampton, Virginia

and

C. Tung**
Aeromechanics Laboratory, AVSCOM
NASA Ames Research Center
Moffett Field, California

Abstract

An efficient finite-difference scheme for the solution of the incompressible Navier-Stokes equation is used to study the vortex wake of a rotor in hover. The solution procedure uses a vorticity-stream function formulation and incorporates an asymptotic far-field boundary condition enabling the size of the computational domain to be reduced in comparison to other methods. The results from the present method are compared with experimental data obtained by smoke flow visualization and hot-wire measurements for several rotor blade configurations.

Introduction

Vortex-dominated flow fields are frequently encountered in the flight operation of fixed- and rotary-wing aircraft. Complete prediction of the flow field is very difficult because of the disparate length scales associated with the generation, interaction, and eventual decay of the vortices. Methods which assume the vortex interactions to be inviscid and represent the flow-field as a series of point or line vortices have proven very useful. Unfortunately, they suffer from the disadvantage of not being able to realistically model either the vortex core or the merging of vortices. Computational methods that solve the Navier-Stokes equations have demonstrated the ability to represent the continuous vorticity distribution that exists within the vortex core as well as the merging characteristics of multiple vortices. However, these methods suffer from the disadvantage of requiring large computer times and storage resources along with restrictions to low Reynolds number flow. Recently, some progress has been made towards an efficient solution procedure for solving the incompressible Navier-Stokes equations[1,2,3]. The procedure uses a vorticity - vector velocity potential formulation and incorporates an asymptotic far field boundary condition enabling the size of the computational domain to be reduced in comparison to other methods. The procedure has been applied successfully in the numerical solution of interacting vortex rings[2] and the two-dimensional roll up of vortex wakes[3].

The present work is an application of the above procedure to the analysis of vortex wake merging and decay for a rotor in hover. The development in time of the two-dimensional wakes calculated in reference 3 represents the streamwise development of the three-dimensional wake and relies on the assumption that streamwise gradients are small. By making an analogous assumption in the case of a rotor in hover that the circumferential gradients are small, the streamwise development of the vortex wake can be reduced to a time-dependent axisymmetric calculation. Results from the continuous vorticity field method can be used to improve the free wake models currently used in prediction methods for helicopter rotor aerodynamic loading[4,5,6]. These methods usually employ a large number of straight-line vortex segments to simulate the shed vorticity in the wake and always contain some empiricism in determining the details of vortex merging as occurs in the roll up of the trailing vorticity in the free wake.

A description of the governing equations and numerical procedure along with some computational results are presented below. Results from the present method are then compared with the experimental data obtained by smoke flow visualization and hot-wire measurements[7].

Governing Equations

The flow is assumed to be governed by the incompressible laminar Navier-Stokes equations. Using a fixed inertial frame with cylindrical coordinates r, θ, and z (r and θ define the plane of the rotor rotation about the vertical axis z)

---

* Research Scientists, Analytical Methods Branch, Low-Speed Aerodynamics Division. Members AIAA.

** Research Scientist, U.S. Army Aeromechanics Laboratory. Member AIAA.

with corresponding inertial velocities u, v, and w, the flow field induced by a rotor in hover is unsteady and three-dimensional. The flow field appears steady and three-dimensional after transformation to a non-inertial frame rotating with the rotor blade as below

$$\begin{aligned} r &= r \\ \phi &= \theta - \Omega t \\ z &= z \\ t &= t \end{aligned} \qquad (1)$$

The rotor blade rotates with angular rate Ω about the z axis and corresponds to ϕ = constant. The three-dimensional flow field can be reduced to an unsteady axisymmetric flow field by assuming (1) the circumferential velocity component and pressure gradient are zero and (2) the rate of change of the velocity gradients in the circumferential direction are small as below

$$v = \frac{1}{r}\frac{\partial p}{\partial \phi} = \frac{1}{r^2}\frac{\partial^2 u}{\partial \phi^2} = \frac{1}{r^2}\frac{\partial^2 w}{\partial \phi^2} = 0 \qquad (2)$$

This assumption is a straight-forward extension of a practice commonly used in fixed-wing analyses to reduce the steady three-dimensional vortex wake roll-up calculation to an unsteady two-dimensional calculation. The development in time of the two-dimensional (in the case of fixed wing) or axisymmetric (in the case of a rotor in hover) flow field represents the streamwise development of the three-dimensional flow. The resulting axisymmetric continuity and momentum equations are given below

$$\frac{1}{r}\frac{\partial}{\partial r}(ru) + \frac{\partial w}{\partial z} = 0 \qquad (3)$$

$$-\Omega\frac{\partial u}{\partial \phi} + u\frac{\partial u}{\partial r} + w\frac{\partial u}{\partial z} = \frac{-1}{\rho}\frac{\partial p}{\partial r} + \nu\left(\nabla^2 u - \frac{u}{r^2}\right) \qquad (4)$$

$$0 = \frac{-1}{\rho r}\frac{\partial p}{\partial \phi} \qquad (5)$$

$$-\Omega\frac{\partial w}{\partial \phi} + u\frac{\partial w}{\partial r} + w\frac{\partial w}{\partial z} = \frac{-1}{\rho}\frac{\partial p}{\partial z} + \nu\left(\nabla^2 w\right) \qquad (6)$$

where the axisymmetric Laplacian operator is

$$\nabla^2 = \frac{1}{r}\frac{\partial}{\partial r}\left(r\frac{\partial}{\partial r}\right) + \frac{\partial^2}{\partial z^2} \qquad (7)$$

Note the above equations are time-like in the variable $-\phi/\Omega$ representing circumferential development of the flow. The above equations can be efficiently solved in vorticity-stream function form as below

$$-\Omega\frac{\partial \zeta}{\partial \phi} + \frac{\partial}{\partial r}(u\zeta) + \frac{\partial}{\partial z}(w\zeta) = \nu\left[\nabla^2\zeta - \frac{\zeta}{r^2}\right] \qquad (8)$$

$$\nabla^2\psi - \frac{2}{r}\frac{\partial \psi}{\partial r} = \zeta r \qquad (9)$$

The vorticity is defined as

$$\zeta = \frac{\partial u}{\partial z} - \frac{\partial w}{\partial r} \qquad (10)$$

and the velocities are obtained as

$$u = \frac{-1}{r}\frac{\partial \psi}{\partial z} \qquad w = \frac{1}{r}\frac{\partial \psi}{\partial r} \qquad (11)$$

The assumption that v = 0 essentially limits the analysis to locations outside the boundary layer near the rotor blade. Note that the no-slip condition on the rotor blade corresponds to $v = +\Omega r$. Equations (8) and (9) correspond to an initial value problem and hence the vorticity must be initialized at $\phi = 0$, corresponding physically to a location a small distance circumferentially downstream of the rotor blade trailing edge. The initial vorticity distribution must be obtained by other means such as experiment or numerical lifting line theory. The rotor blade loading is used to determine the initial vorticity and a comparison of rotor blade loading obtained from experiment[7] with that obtained from lifting surface theory[4] for a two-bladed rotor (radius/chord = 6.0) is shown in figure 1.

Computational Method

The actual helical pattern of the shed vorticity is approximated by a series of axisymmetric vorticity distributions. Their respective vertical locations correspond to that which would be obtained by passing a plane ϕ =constant through the rotor downwash field as shown in figure 2.

The boundary conditions used in the far field away from the downwash field directly below the rotor are

$$u^2 + w^2 = O(d^{-2}) \quad \text{as} \quad d = (r^2+z^2)^{1/2} \to \infty \qquad (12)$$

$$\zeta = O(e^{-d^2}) \quad \text{as} \quad d = (r^2+z^2)^{1/2} \to \infty \qquad (13)$$

corresponding to the vorticity distribution being of finite extent and having a distribution analagous to a classical Lamb vortex. As pointed out in references 1 and 2, the condition (13) is much stronger than (12) and a substantially more accurate solution can be obtained by imposing (13) and solving (8-9) rather than imposing (12) and solving (3-6) on any bounded domain.

The vorticity transport equation is solved on the bounded domain D as shown in figure 2 subject to the boundary condition $\zeta = 0$ on the outer boundary. The wake structure outside of the domain D has reached an asympotic state and could be approximated as a series of Lamb vortices. The movement and diffusion of these vortices could then be calculated by an asymptotic analysis as in reference 2 and their influence on the velocity field in D calculated exactly. For the present

results, however, the vorticity distribution is contained entirely within the bounded domain D. The vorticity is initialized at $\phi = 0$ from the prescribed rotor loading distribution and at intervals in time corresponding to the circumferential distance from one blade passage to another, the initial distribution of vorticity is superimposed on the existing vorticity distribution. The interval in time between blade passages corresponds to $\phi = \pi$ for a two-bladed rotor. The vertical separation of the superimposed vorticity distribution is obtained from experiment as discussed subsequently. Results have been obtained for up to 8 superpositions of initial vorticity corresponding to 4 rotor revolutions for a two-bladed rotor.

The velocity due to the vorticity field in D is calculated by using a fast Poisson solver to solve equation (9) for ψ and differentiating as in equation (11). The exact integral equation relating velocity to vorticity (usually referred to as the Biot-Savart relationship) could be integrated numerically to obtain the stream function in the computational domain. However, numerical integration of this equation over the entire flow field requires at least $O(N^4)$ operations where N is a typical number of computational grid points along either r or z. Numerically integrating to find only the boundary values requires $O(N^3)$ operations. Using a far-field representation for the boundary values of ψ as derived in references 1 and 2 requires only $O(N^2)$ operations. The far-field expansion uses moments of the vorticity distribution as given below

$$\psi(r,z,\phi) = \frac{1}{4d}\left(\frac{r}{d}\right)^2 \{ \langle \zeta r'^2 \rangle + \frac{3}{d}\left(\frac{z}{d}\right) \langle \zeta r'^2 z' \rangle + \frac{3}{2d^2} \left[5\left(\frac{z}{d}\right)^2 - 1\right] \langle \zeta r'^2 z'^2 \rangle + \left[\frac{5}{4}\left(\frac{r}{d}\right)^2 - 1\right] \langle \zeta r'^4 \rangle] \} + O(d^{-4}) \quad (14)$$

where the moments of vorticity are defined as

$$\langle \zeta r'^m z'^n \rangle \equiv \int_{-\infty}^{\infty} \int_0^{\infty} \zeta(r',z',\phi)\, r'^m\, z'^n\, dr'\, dz' \quad (15)$$

Note the second moment of vorticity $\langle \zeta\, r'^2 \rangle$ is known to be conserved and hence can be used to measure the error of the numerical solution. Since evaluation of ψ using the fast Poisson solver requires only O(NlnN) operations, the resulting procedure represents a very efficient method of solving the incompressible Navier-Stokes equations.

Results and Discussion

Results using the procedure applied to a representative loading distribution shown in figure 3 are discussed below. The corresponding initial vorticity distribution was generated by summing a series of individual Lamb vortices along the computational grid as in reference 3. The strengths of the Lamb vortices are determined by the change in load distribution between grid points with the core radius of each vortex prescribed to be a fixed percentage (in this case, 2.5 percent) of the rotor radius R.

In figure 4, the distribution of vorticity at several circumferential positions $(-\phi/2\pi)$ downstream of the rotor blade are shown for a Reynolds number based on Ω and rotor radius R of 40,000. The roll up and inboard movement of the vorticity occurs very rapidly and the merging is almost complete by one revolution. Note these calculations were made without including the influence of the shed vorticity beneath the plane of rotor.

The effect of the asymptotic far-field boundary condition procedure is shown in figure 5. The $\psi = 0$ boundary condition clearly shows the effect of the finite grid extent. Imposing the far field boundary condition using $\psi = 0$ with an equivalent accuracy to the far field expansion procedure would require a much larger grid size with a subsequent loss of accuracy for the interior finite difference calculations assuming the practical restraint of a fixed number of grid points.

The grid size used for high Reynolds number flow computation is required to be very fine to be compatible with the wake thickness at high Reynolds number which, in the experimental data[7], was on the order of 0.003R. The computational time increases as Reynolds number increases and wake thickness decreases. In the following, all the computations were done at Reynolds number equal to 40,000 and the wake thickness was taken as 0.025R as a trade-off between computer time and storage. The grid size was constant in both the radial and axial directions and was equal to 0.0125R. The number of grid points was 100 and 200 in the radial and axial directions, respectively, and required approximately 1 hour computational time on a VAX 11/780 computer to predict nine revolutions of the rotor.

The present method has been applied to three different test in which the wake geometries were measured by a hot-wire sensor. The first case[8] considered is a single blade rotor with aspect ratio equal to 4.8 operating at a collective pitch angle equal to 6.2 and rotational speed equal to 1350 revolutions per minute. The experimental tip vortex path (figures 6 and 7) shows a good correlation with Landgrebe's empirical formula[9]. To include the influence of the shed vorticity beneath the plane of the rotor, as discussed above, a new layer of vorticity of the same

strength and distribution as the initial vorticity has been generated at the plane of the rotor at the time of blade passage. The axial separation was determined from the experimental data shown in figure 6. The computation has been carried out for nine revolutions. The vorticity distribution computed by using a lifting surface code[4] is presented in figure 8 as well as in Table I of the Appendix. Comparisons of experiment and lifting surface calculations[4] for the rotor loading for all three rotors studied have been similar to that shown in figure 1 and, for all the calculations presented, the lifting surface calculations have been used to determine the rotor loading.

The vorticity at the end of each blade passage was about 60% of its original value and thus the mutual interaction has been dominated by the new vorticity. The first concentrated vorticity has been pushed out more in the radial direction while the second one moves inboard slightly. As new distributions of vorticity were generated due to blade passage, the first concentrated vorticity moved outward more and more as shown in figure 9. However, the concentrated vorticity nearest the plane of the rotor did not move inboard enough to match the test data which were obtained at high Reynolds number condition. The Reynolds numbers of the experiments are .5 X 10^6 and .75 X 10^6 for the single- and the two-bladed rotors, respectively. The predicted wake geometry did not agree with the measurements but the general trend was encouraging. The source of disagreement may be attributed to either the low Reynolds number or the time-dependent nature of the present calculations which have not yet reached a steady state condition. It is believed, however, that the low Reynolds number in the calculations are the predominant source of the disagreement. Computations approaching the high Reynolds number flow condition could be achieved by using a multi-scale technique in which a fine grid is used around the concentration of vorticity while a coarse grid is used for the general flow domain. This technique is currently under development by the present authors.

The second and third cases considered are two-bladed rotors, one with aspect ratio equal to 6.0 (FXC blade) and the other with an aspect ratio equal to 13.7 (1/7-Scale UH-1 blade). The vorticity distribution of each case is shown in figures 10 and 11 as well as in Table II and III, respectively, of the Appendix.

Smoke visualization photographs showing the movement and interaction of the tip vortex cores are shown in figures 12 and 13 for the AR = 13.7 blade. The motion and decay of the shed vorticity for each case are shown in figures 14 and 15 and show similar trends to that discussed previously.

Concluding Remarks

An efficient finite-difference scheme for the solution of the incompressible Navier-Stokes equations has been used to study the vortex wake of a rotor in hover. The present method has been applied to three different tests in which the wake geometries were measured by the hot-wire sensor. Comparisons show that the computed concentrated vorticity nearest the plane of the rotor did not move inboard enough to match the test data, but the general trend of the predicted wake geometry was encouraging. The source of disagreement may be attributed to either the time-dependent nature of the present calculations which have not yet reached a steady state condition or the low Reynolds number. It is believed, however, that the low Reynolds number in the calculations are the predominant source of the disagreement. The difficulty in computing the high Reynolds number flow condition could be eliminated by using a multi-scale technique in which a fine grid is used around the concentration of vorticity and a coarse grid for general flow domain. This technique is currently under development.

References

1. Ting, L.: "On the Application of the Integral Invariants and Decay Laws of Vorticity Distributions," Journal of Fluid Mechanics, Vol. 127, February 1983, pp. 497-506.

2. Liu, C. H., and Ting, L., "Numerical Solution of Viscous Flow in Unbounded Fluid," Lecture Notes in Physics, Vol. 170, Eighth International Conference on Numerical Methods in Fluid Dynamics, Proceedings, Aachen 1982, Springer-Verlag, pp. 357-363.

3. Weston, R. P.; and Liu, C. H.: "Approximate Boundary Condition Procedure for the Two-Dimensional Numerical Solution of Vortex Wakes," AIAA Paper No. 82-0951, presented at the AIAA/ASME 3rd Joint Thermophysics, Fluids, Plasma, and Heat Transfer Conference, June 1982, St. Louis, Missouri.

4. Summa, J. F., "Advanced Rotor Analysis Methods for the Aerodynamic Blade/Vortex Interaction in Hover," Paper No. 28, presented at the 8th European Rotorcraft Forum, Ex-en-probence, France, August 1982.

5. Miller, R. H.: "A Simplified Approach to the Free Wake Analysis of a Hovering rotor," VERTICA, Vol. 6, 1982, pp. 89-95.

6. Stremel, P. M.: "Computational Methods for Non-planar Vortex Wakes Flow Fields with Applications to Conventional and Rotating Wings," M.S. Thesis, MIT, February 1982.

7. Tung, C., et al.: "The Structure of Trailing Vortices Generated by Model Rotor Blades," NASA TM 81316, August 1981.

8. Shivananda, T. P., "Pressure Measurements Near the Tip of a Hovering Model Rotor Blade and a Preliminary Investigation of the Flow in the Rotor Wake", Ph.D. thesis, Georgia Institute of Technology, Dec. 1977.

9. Landgrebe, A. J., "An Analytical and Experimental Investigation of Helicopter Rotor Hover Performance and Wake Geometry Characteristics", USAAMRDL TR 71-24, June 1971.

Appendix

Table I. Georgia Tech Single Blade, AR = 4.8
$\theta_c = 6.2^0$, R = 2 ft., Ω = 1,350 rpm

r/R	0.0	.15	.275	.325	.5
$\Gamma/\Omega R^2$	0.0	0.0	.00589	.00833	.0134
r/R	.683	.735	.775	.805	.845
$\Gamma/\Omega R^2$	.0191	.0211.	.0227	.0238	.0249
r/R	.885	.91	.92	.94	.96
$\Gamma/\Omega R^2$	.0249	.0241	.0236	.0222	.0203
r/R	.98	.987	.991	.995	.998
$\Gamma/\Omega R^2$	.0183	.0179	.0180	.0183	.0187
r/R	1.0				
$\Gamma/\Omega R^2$	0.0				

where θ_c is collective pitch angle.

Table II. FXC AR = 6.0 Blade
$\theta_c = 8^0$, R = 3.75 ft., Ω = 1,250 rpm

r/R	0.0	0.144	0.222	0.375	0.525
$\Gamma/\Omega R^2$	0.0	0.0	0.00344	0.00643	0.00997
r/R	0.650	0.750	0.810	0.830	.0850
$\Gamma/\Omega R^2$	0.0137	0.0173	0.0199	0.0215	0.0229
r/R	0.870	0.890	0.910	0.930	0.950
$\Gamma/\Omega R^2$	0.0241	0.0252	0.0258	0.0259	0.0252
r/R	0.970	0.988	1.0		
$\Gamma/\Omega R^2$	0.0235	0.0221	0.0		

Table III. 1/7-Scale Huey Blade, AR = 13.7
$\theta_c = 8^0$; R = 3.43 ft., Ω = 1,250 rpm

r/R	0.0	.144	.222	.375	.525
$\Gamma/\Omega R^2$	0.0	0.0	.00406	.00621	.00881
r/R	.65	.75	.81	.83	.85
$\Gamma/\Omega R^2$	.0113	.0135	.0151	.0162	.0175
r/R	.87	.89	.91	.93	.95
$\Gamma/\Omega R^2$	.0188	.0199	.0205	.0203	.0191
r/R	.97	.988	1.0		
$\Gamma/\Omega R^2$	.0165	.0125	0.0		

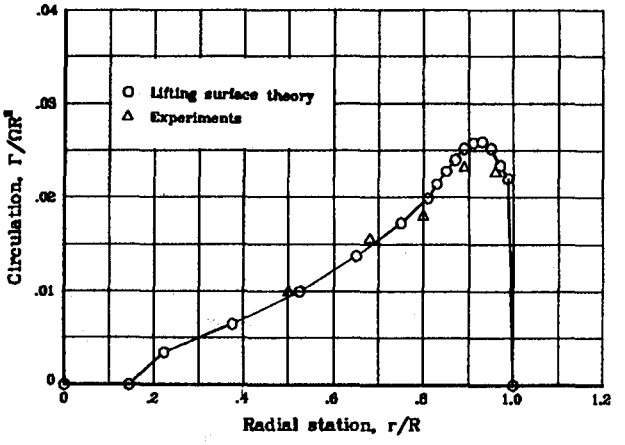

Figure 1.- Comparison of experimental rotor loading with lifting surface theory for a two-bladed rotor (AR = 6.0).

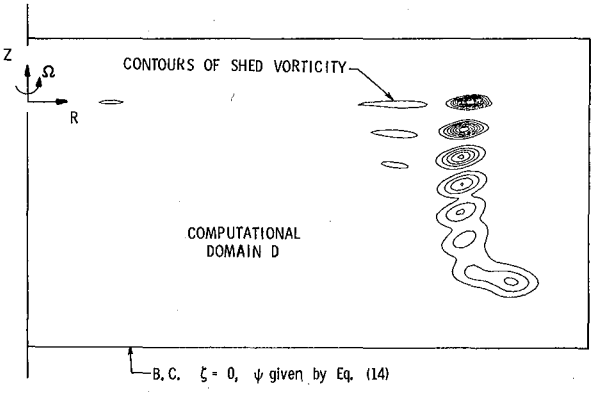

Figure 2.- Bounded domain used in rotor wake analysis.

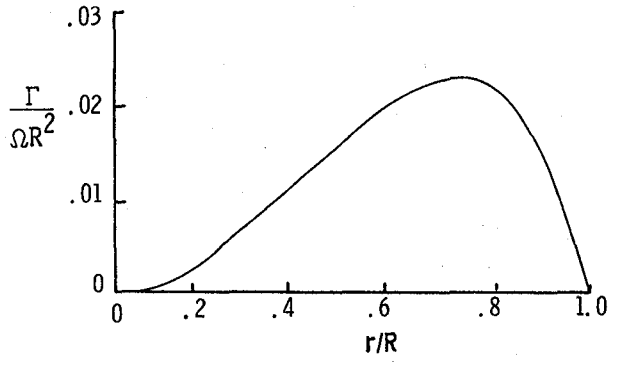

Figure 3.- Initial load distribution used in numerical experiments for vorticity evolution computations.

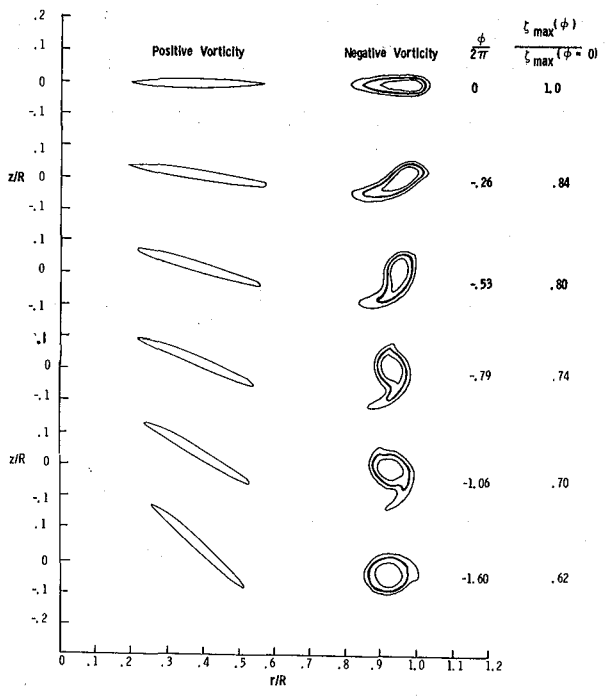

Figure 4.- Streamwise development of vorticity for initial load distribution shown in figure 3.

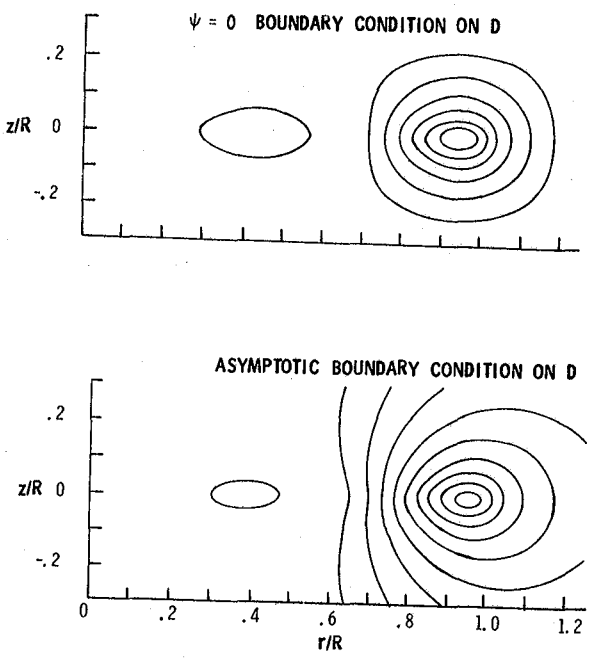

Figure 5.- Effect of far-field boundary condition.

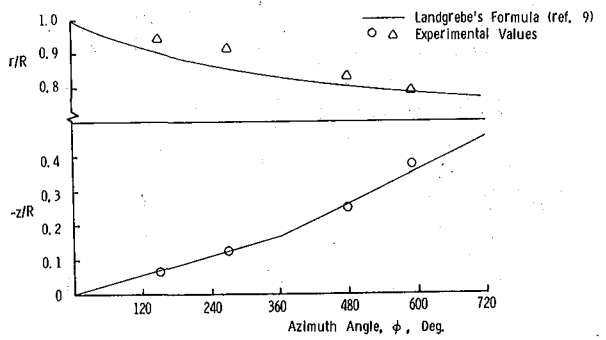

Figure 6.- Comparison of experimental tip vortex geometry with empirical geometry for AR = 4.8 single-bladed rotor.

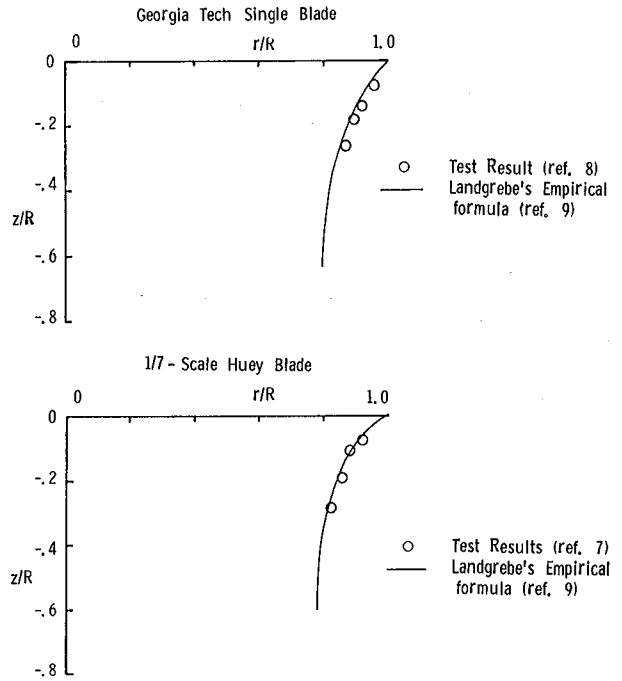

Figure 7.- Inboard movement of tip vortex paths for single and two-bladed rotors.

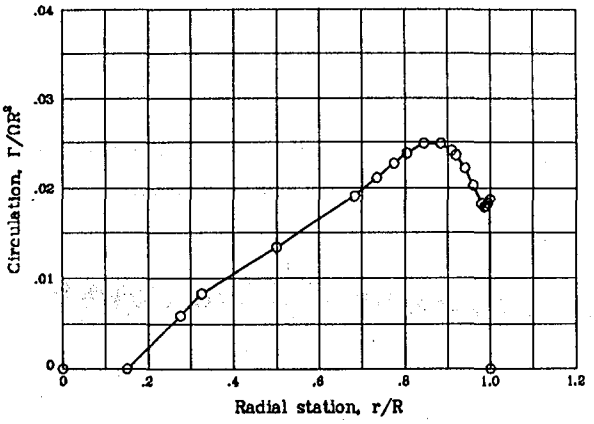

Figure 8.- Blade sectional loading for Georgia Tech single blade, AR = 4.8.

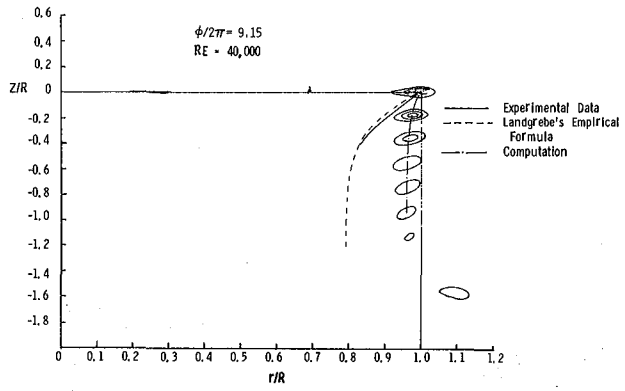

Figure 9.- Comparison of experimental tip vortex path locations with present results for an AR = 4.8 single-bladed rotor.

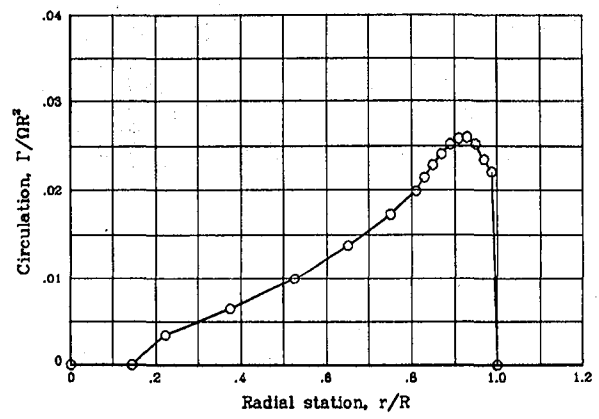

Figure 10.- Blade sectional loading for AR = 6 two-bladed rotor.

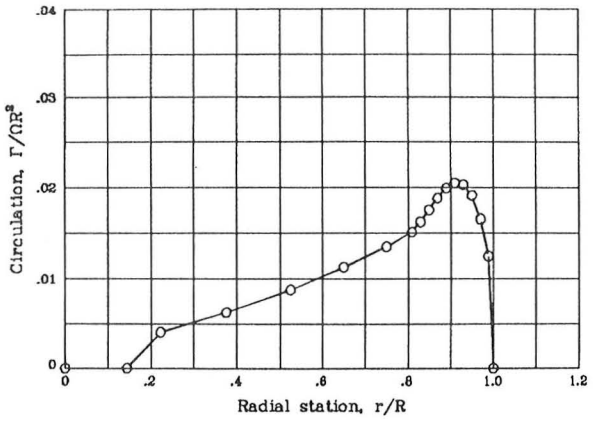

Figure 11.- Blade sectional loading for 1/7 - scale Huey blade, AR = 13.7.

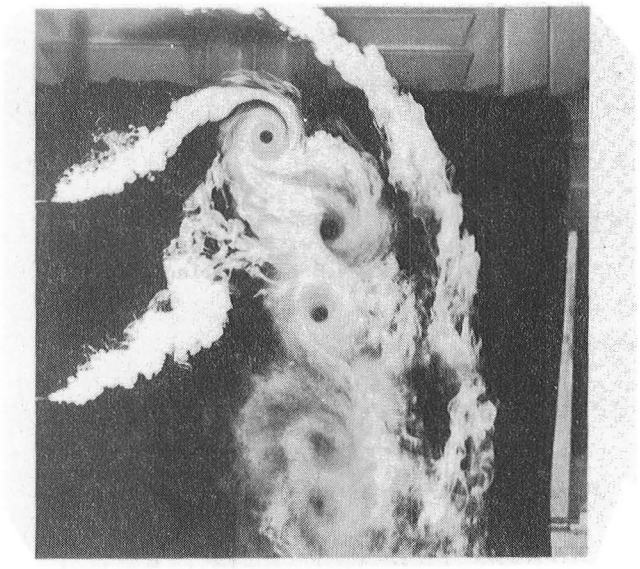

Figure 12.- Smoke Visualization. AR = 13.7, 1/7 - scale untwisted Huey blade.

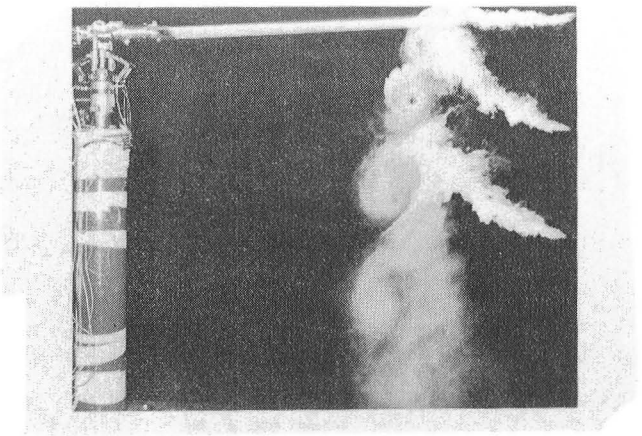

Figure 13.- Smoke Visualization. AR = 13.7, 1/7 - scale untwisted Huey blade.

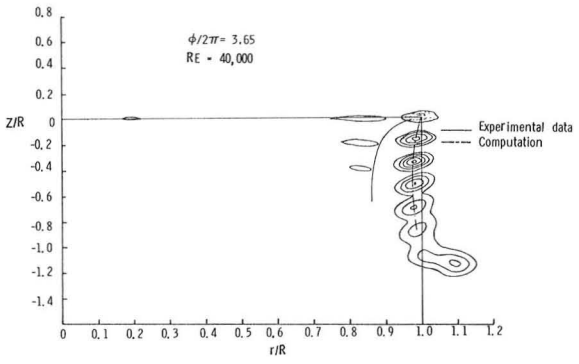

Figure 14.- Comparison of experimental tip vortex path locations with present results for an AR = 6.0 two-bladed rotor.

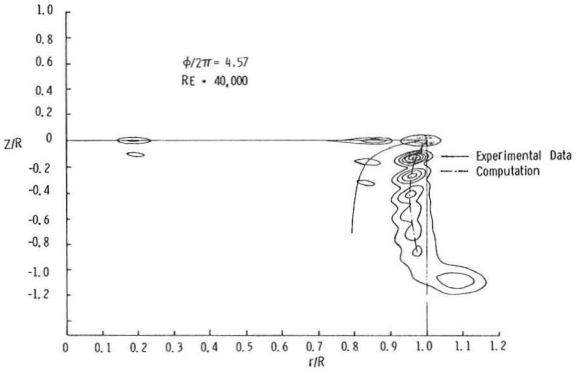

Figure 15.- Comparison of experimental tip vortex path locations with present results for an AR = 13.7 two-bladed rotor.

1. Report No.	2. Government Accession No.	3. Recipient's Catalog No.
NASA TM-85894		

4. Title and Subtitle	5. Report Date
NAVIER-STOKES CALCULATIONS FOR THE VORTEX WAKE OF A ROTOR IN HOVER	May 1984
	6. Performing Organization Code
7. Author(s) C. H. Liu and J. L. Thomas (Langley Research Center, Hampton, Va.), and C. Tung	8. Performing Organization Report No. A-9611
	10. Work Unit No. K-1585
9. Performing Organization Name and Address Ames Research Center and Aeromechanics Laboratory, U.S. Army Research and Technology Laboratories, AVSCOM, Moffett Field, CA 94035	11. Contract or Grant No.
	13. Type of Report and Period Covered Technical Memorandum
12. Sponsoring Agency Name and Address National Aeronautics and Space Administration, Washington, DC 20546 and U.S. Army Aviation Research and Development Command, St. Louis, MO 93166	14. Sponsoring Agency Code

15. Supplementary Notes

Point of Contact: C. Tung, Ames Research Center, MS 215-1, Moffett Field, CA 94035 (415) 965-5892 or FTS 448-5892

16. Abstract

An efficient finite-difference scheme for the solution of the incompressible Navier-Stokes equation is used to study the vortex wake of a rotor in hover. The solution procedure uses a vorticity-stream function formulation and incorporates an asymptotic far-field boundary condition enabling the size of the computational domain to be reduced in comparison to other methods. The results from the present method are compared with experimental data obtained by smoke flow visualization and hot-wire measurements for several rotor blade configurations.

17. Key Words (Suggested by Author(s))	18. Distribution Statement
Navier-Stokes equations Vortex	Unlimited Subject Category - 02

19. Security Classif. (of this report)	20. Security Classif. (of this page)	21. No. of Pages	22. Price*
Unclassified	Unclassified	11	A02

*For sale by the National Technical Information Service, Springfield, Virginia 22161